BULLETIN OF THE POLISH ACADEMY OF SCIENCES TECHNICAL SCIENCES, Vol. 73(6), 2025, Article number: e155045 DOI: 10.24425/bpasts.2025.155045

MECHANICAL AND AERONAUTICAL ENGINEERING, THERMODYNAMICS

Material and technological concept of the construction of a turboshaft engine with the application of isochoric combustion – CFD thermal analysis

Piotr TARNAWSKI®*

Division of Numerical Methods and Intelligent Structures, Warsaw University of Technology, ul. Narbutta 84, 02-524 Warsaw, Poland

Abstract. The paper presents the concept of a turboshaft engine with the application of isochoric combustion, along with its technological design and the selection of construction materials. The presented engine concept and construction design are based on a three-dimensional numerical CFD analysis. The first stage of analysis concerned the development of the construction of the valve timing system itself. This simplified model of the engine can be used for the experiential verification of the self-adjusting segmented ceramic sealing system, which is an integral part of the presented engine concept. The second stage of analysis concerned the development of the construction of a prototype engine. To ensure high engine efficiency, it was necessary to provide a high temperature of gas in combustion chambers, and at the same time limit heat losses. The application of ceramics, as a construction material for chambers and nozzles, was a choice since it is resistant to high temperatures. To reduce heat losses, the area of contact between hot engine components was limited. Moreover, the implementation of screens reduced heat transfer by radiation. Finally, polishing the surfaces facilitated a reduction of radiation coefficients. The analysis conducted demonstrated that it is possible to construct an engine with promising effective efficiency and ensure that materials work below permissible temperatures.

Keywords: isochoric combustion; Humphrey cycle; turboshaft engine; CFD analysis; sealing system.

1. INTRODUCTION

Despite the growing popularity of electromobility and hydrogen drive, the demand for a competitive turboshaft engine with internal combustion is great. There are no real prospects now for the next decade or two for using an alternative drive to the combustion engine for heavy vehicles or turboprops, which require efficient operation over long distances. The existing problems of electric vehicles are worth noting [1,2]. Low electricity density requires the construction of large and heavy batteries, which prove to be questionable when it comes to use in flying objects. The issue of hydrogen drive as a technology is at an early stage of advancement, not to mention the infrastructure for refueling and hydrogen electrolysis plants, which in practice do not exist [3,4].

In contrast, the development of ecological fuel production technology is promising. Shortly, it could replace classic hydrocarbons used in combustion engines. Thanks to the newly developed method of synthesis of liquid hydrocarbons, it is possible to easily process catalytically glycerol into suitable chemical substances, which can be used as "ecological" fuel for combustion engines. Synthesized hydrocarbons such as alkanes can become an alternative to currently used fuels produced from crude oil [5,6].

To reduce environmental pollution generated by an aircraft application, great hopes are placed on pressure gain combustion

Manuscript submitted 2025-03-26, revised 2025-07-02, initially accepted for publication 2025-08-04, published in November 2025.

(PGC) [7–12], where the basic thermodynamic cycle can be enhanced. The pressure gain combustion process can be conducted by combustion in a constant volume chamber or by detonating combustion.

The paper presents the engine concept with isochoric combustion and the results of CFD simulation of engine work and its effective efficiency. The technological design and selection of construction materials were conducted as a second step. The thermal analysis and temperature distribution were used as primary tools. Three heat transfer modes were considered in the simulation: conduction, convection, and radiation. In the first stage, the engine timing system itself was constructed. This simplified model of the engine would be used for experimental verification of the proposed sealing system. In the second step, the construction of the entire engine was developed, with the research tool being a numerical simulation.

2. DESCRIPTION OF METHODOLOGY

The geometry model of the engine was developed step by step, gradually removing its defects. The simulation model made it possible to evaluate the engine performance and to introduce resulting improvements. The 3D numerical analysis contained a simulation of filling, direct injection of fuel, isochoric combustion, expansion, and mechanical power generation in the turbine. A transient set of Navier-Stokes equations, together with a compressible, semi-ideal energy equation, species transport, and reaction of combustion, was resolved. The thermal properties of gas species (specific heat, thermal conductivity, viscosity) were temperature dependent. The commercial ANSYS Fluent

^{*}e-mail: piotr.tarnawski@pw.edu.pl

software was employed for analysis. The detailed numerical approach is given in the author's previous papers [13, 14].

3. THE EFFICIENCY OF THE ENGINE CONCEPT WORKING ACCORDING TO THE HUMPHREY CYCLE

Implementation of the isochoric combustion can increase the efficiency of the thermodynamic cycle from 0.56 to 0.66 (see a comparison of the Humphrey cycle versus the Bryton-Joule cycle in Fig. 1). However, the realization of the Humphrey cycle requires ensuring temporary closing and opening of combustion chambers. The systematically developed engine concept presented in the paper includes the timing system based on mutually rotating elements [13, 14] (see simulation model in Fig. 2 and its mesh in Fig. 3). The engine cycle consists of a filling of externally compressed fresh air, isochoric combustion, and high-pressure exhaust. It was realized by the implementation of rotating combustion chambers, working together with a stationary nozzle (see simulation model and results in Figs. 3 and 4). Due to the use of isochoric combustion, the pressure value in the chamber reached 5.3 MPa, at a compression pressure equal to 2.0 MPa (Fig. 5). The moment generated in turbine, for symmetrically half of the engine, is presented in Fig. 6. The effective efficiency of the engine evaluated by CFD simulation reached 31.8% for 439.1 kW and 34.5% for 1000 kW [15]. The results are extremely promising since its efficiency exceeds the efficiency of classical turboshaft engines available in the market, e.g., the PWD207D - 427 kW has an efficiency equal to

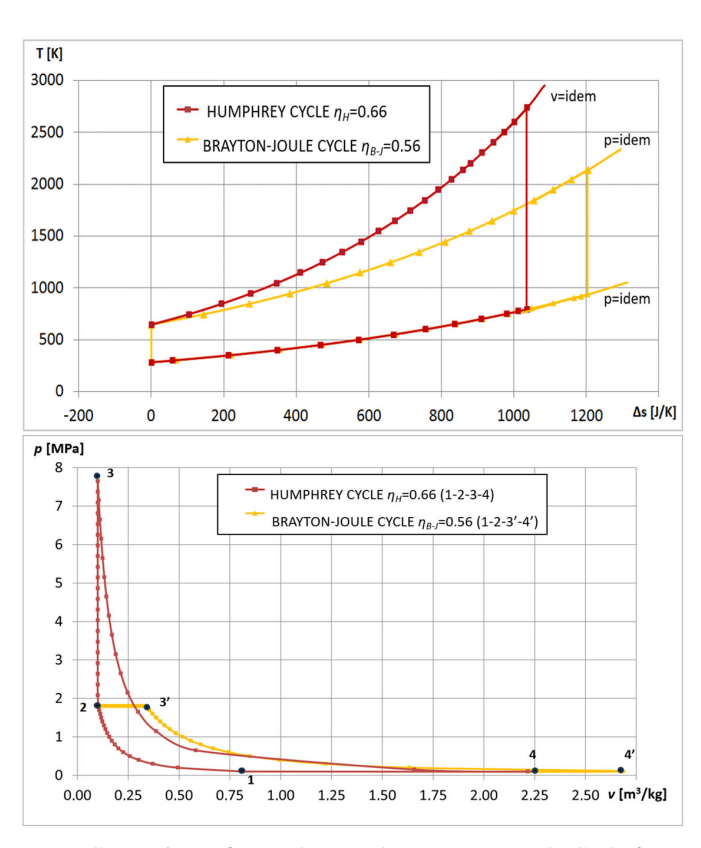


Fig. 1. Comparison of Humphrey cycle vs. Bryton-Joule Cycle for T-s coordinate system (top picture) and p-v coordinate system (bottom picture)

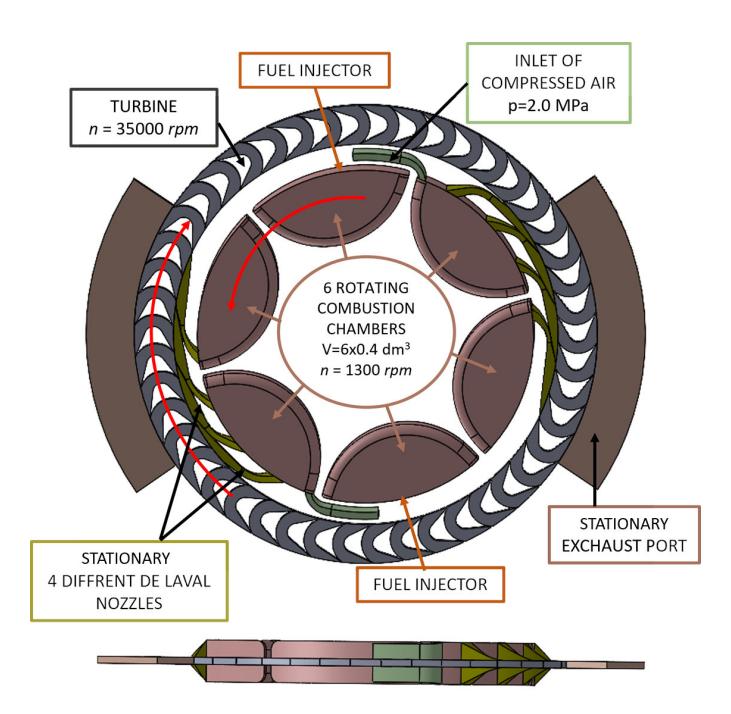


Fig. 2. Simulation model of turboshaft engine concept with – 500 kW (general and top view)

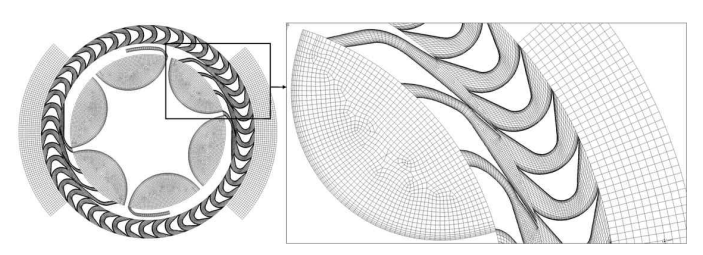


Fig. 3. Numerical mesh of the CFD simulation model of the engine

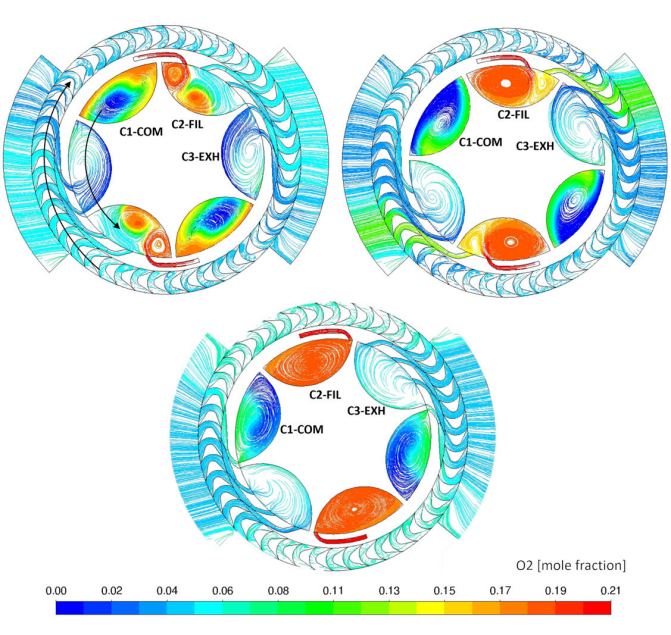


Fig. 4. Change in oxygen content of the gas for 60 degrees of rotation of chambers (one engine cycle)

Material and technological concept of the construction of a turboshaft engine with the application of isochoric combustion...

25.1% and the MTR390 – 958 kW has an efficiency equal to 29.3% [16]. An effective realization of the Humphrey cycle was ensured by:

- Exhaust the remaining part of the gas from the combustion chambers and almost isobaric filling (Fig. 5).
- The continuity of gas flow in the nozzles and the turbine despite the pulsating character of the engine.
- The expansion of gas in different pressure nozzles.
- The setting of the nozzles at different angles according to the turbine.
- The implementation of a turbocharger, using the rest of the kinetic energy behind the main turbine.

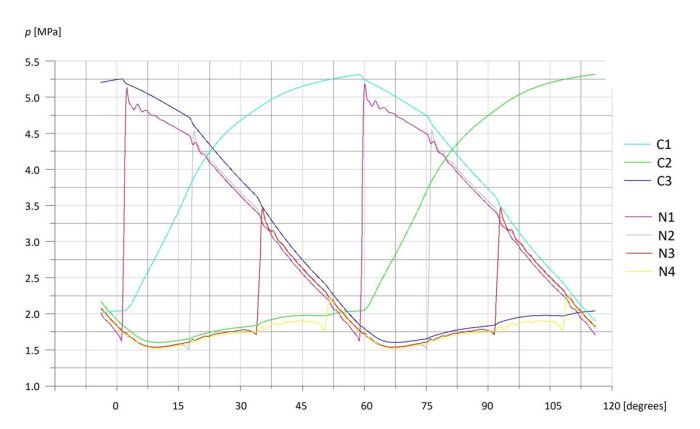


Fig. 5. Pressure changes in combustion chambers and nozzles for two engine cycles (C1, C2, C3 – chambers, N1–N4 – nozzles)

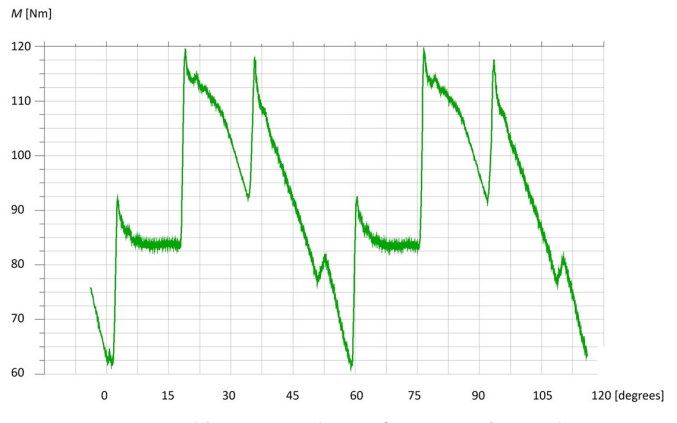


Fig. 6. Turbine torque change for two engine cycles

It is worth mentioning the simplicity of the presented engine concept. It consists of a two-stage compression (turbo-compressor and centrifugal compressor (Fig. 7). Only two sets of high-pressure injection systems are required. The power is generated in a one-stage turbine. Moreover, the injection system and turbochargers universally available in the automotive market can be adopted [17,18]. The points 4–6 on the diagram (Fig. 7) were analyzed by CFD analysis, using the simulation model shown in Fig. 2. The remaining points were calculated analytically, based on CFD results.

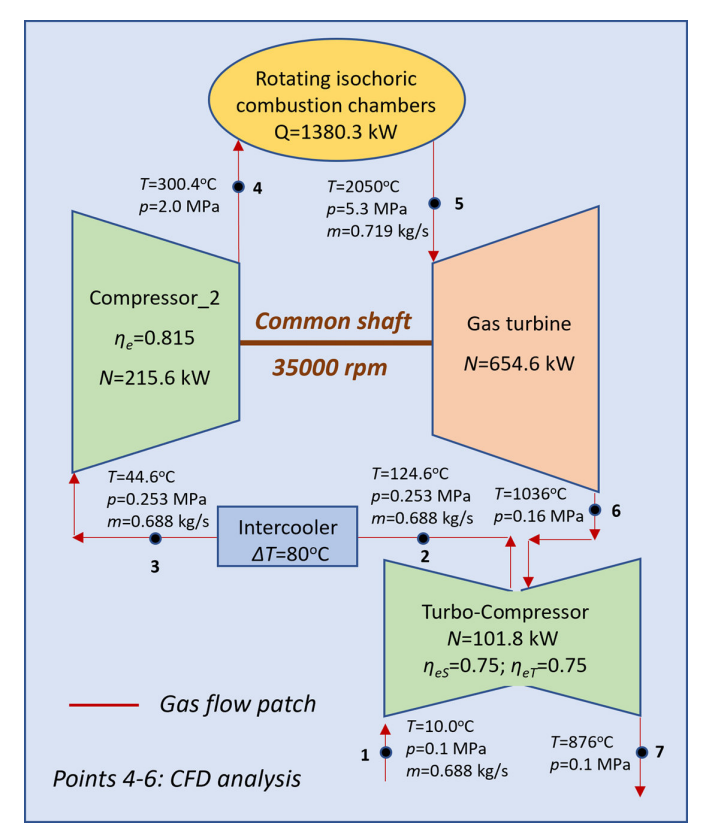


Fig. 7. Diagram of an engine with isochoric combustion

4. THE CONCEPT OF CONSTRUCTION OF THE VALVE TIMING SYSTEM

An integral part of the presented engine concept is a self-adjusting segmented ceramic sealing system [19, 20]. It consists of combustion chambers, segment-sealing elements, and casing. They are made from the same Si3N4 ceramic material, withstanding high temperatures (1300°C) [21] and with a low thermal expansion $(3.2 \cdot 10^{-6})^{\circ}$ C). The sealing system is based on centrifugal force coming from the rotation of combustion chambers. As a result, it can adapt to the size of the changing gap that occurs between chambers and the counter-surface of the casing. It can ensure thickness, regardless of thermal conditions and related deformations.

The proposed sealing system is a critical point in the design of an engine with isochoric combustion chambers. Effective tightness is key to the successful implementation of the Humphrey thermodynamic cycle. The technological details of self-adjusting segmented ceramic sealing systems will be presented in another paper.

The model of the valve timing system shown in Fig. 8 is sufficient for experimental verification of the sealing system [22]. It consists of six combustion chambers driven by an electric motor, a single power supply system (inlet, injector, exhaust, measuring sensors, spark plug), a sealing system, body, base, bearing housing, and bearing.

The parameters for experimental verifications are as follows:

 Achieving a pressure increase in the chambers of at least 2.5 times the compression pressure.

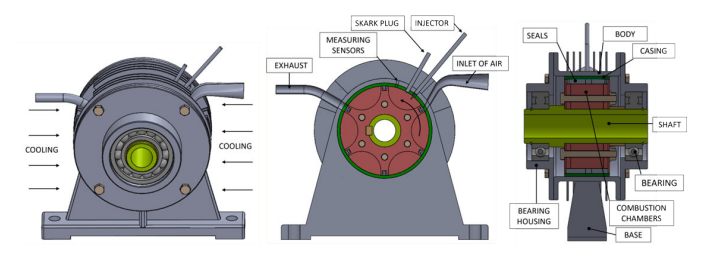


Fig. 8. Geometry model of valve timing system of engine for experimental verification of sealing system

- Achieving a small resistance torque of the seals, generating no more than 2–3% of losses concerning the generated turbine work.
- Achieving the durability of the seals of 600–800 hours of work without the need for replacement.

The main objective of the research was the construction design of a valve timing system and the selection of construction materials. After several modifications, the model shown in Fig. 9 was obtained. There are visible materials and the thermal conductivities of components. The strategy in building the construction was to maintain high temperature in combustion chambers and, at the same time, reduce heat loss and lower the external surface temperature. It is worth mentioning the following implemented steps:

- Reduction of conduction heat transfer by limiting the contact area of the ceramic chambers with the shaft, the ceramic casing with the cast iron casing, and the cast iron casing with the cast iron body.
- Reducing radiative heat transfer by the implementation of screens.
- Reducing radiative heat transfer by polishing the surfaces (reduction of the emissivity factor).
- Enhancing the heat transfer from external surfaces by the implementation of ribs.

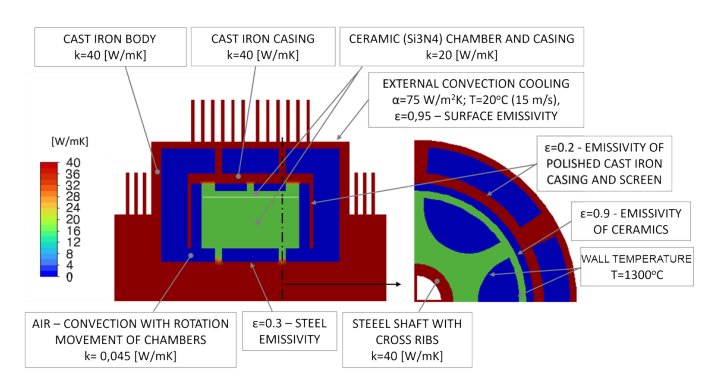


Fig. 9. Construction of valve timing system – selection of materials

The CFD thermal steady state analysis was conducted using ANSYS Fluent software [23] with a mesh consisting of 204 783 hexahedral elements (see Fig. 9).

The structure was heated by a boundary condition of temperature equal to 1300°C. The value was assigned to the inner surface of the chambers. The structure was cooled by forced air movement from the fan. The ambient temperature was equal to

20°C, and the heat transfer coefficient was equal to 75 W/m²K, which corresponded to an air velocity of 15 m/s, blown from the cooling fan (Fig. 10). The resulting temperature of the iron cast was below 1100°C [24], which fulfils the requirements for this material. The temperature of the external body and ends of the shaft was below 250°C (see temperature distribution of construction in Fig. 11), which allows for the shaft bearing. The heat flux of construction cooling was equal to 5340 W. It was 4.3% of fuel chemical energy.

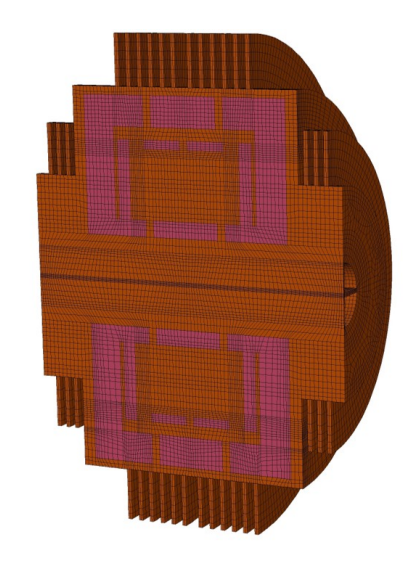


Fig. 10. Numerical mesh of thermal model of valve timing system (orange – solids, pink – air)

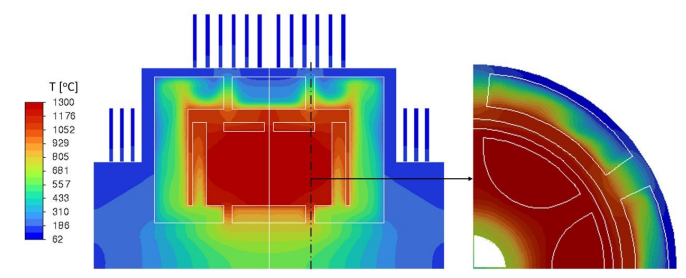


Fig. 11. Temperature distribution of the construction of the valve timing system

5. THE CONCEPT OF THE ENGINE CONSTRUCTION

The presented engine construction has two shafts. The first is responsible for driving the chambers. The second shaft is joined with a turbine; thus, it receives mechanical power (see Fig. 12). The engine needs to be sealed in two locations. The ceramic sealing of combustion chambers and labyrinthine sealing of the turbine are visible. The labyrinth seals can be successfully used in a rotating turbine [25, 26], where the pressure is much lower than in the combustion chambers. For combustion chambers, original ceramic sealing systems were developed, but it is not discussed in detail here.

The CFD thermal analysis of engine construction was conducted step by step [27, 28]. Combustion chambers were built

Material and technological concept of the construction of a turboshaft engine with the application of isochoric combustion...

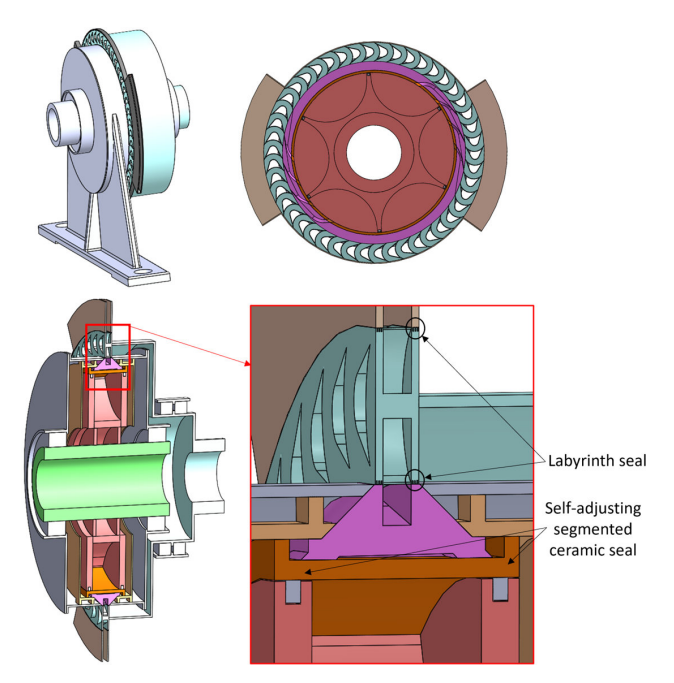


Fig. 12. Geometry model of the construction of the engine prototype

based on knowledge gained from previous analyses of the construction of the valve timing system. Firstly, only the nozzles were added to the simulation model. The body, made previously of cast iron, was changed to aluminum alloy. It has high thermal conductivity, providing a more uniform temperature. After polishing its surface, an extremely low emissivity factor equal to $\varepsilon = 0.05$ could be obtained (Fig. 13). The maximal temperature equal to 1300°C was set as the boundary condition for the internal surface of combustion chambers and internal surface of nozzles. The external forced convection with heat transfer coefficient equal to 75 W/m²K and external temperature 20°C was assumed (Fig. 13). The resulting temperature distribution of construction with nozzles is presented in Fig. 14. The heat flux of cooling chambers was equal to 8016 W, whereas the heat flux of cooling of nozzles was equal to 1796 W. Only heat flux of cooling of chambers met the requirements. The heat flux of cooling, obtained with the simulation model of engine operation presented in Section 3 (Fig. 2), was as follows: for chambers, it was equal to 8140 W, and for nozzles, it was equal to 24363 W (see Fig. 15). The conclusion was that cooling flux of nozzles should be intensified.

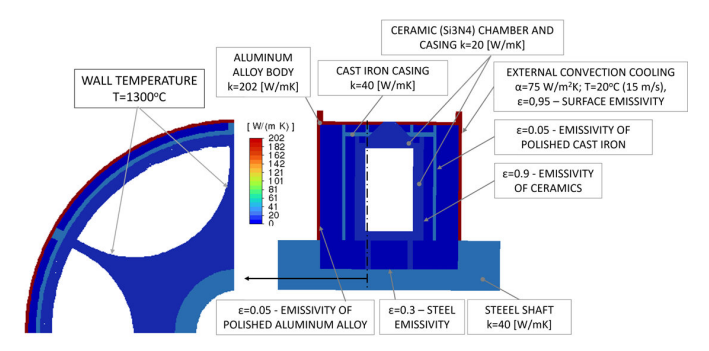


Fig. 13. Construction of engine – selection of materials

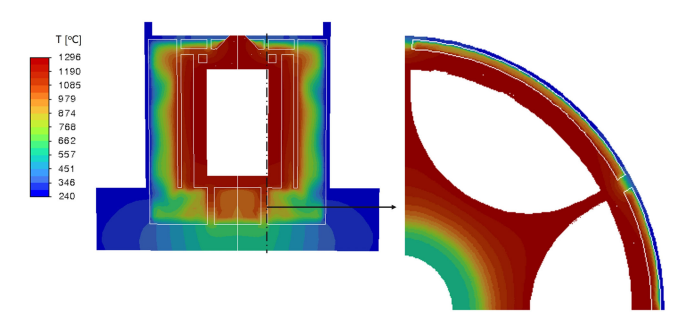


Fig. 14. Temperature distribution of construction with nozzles

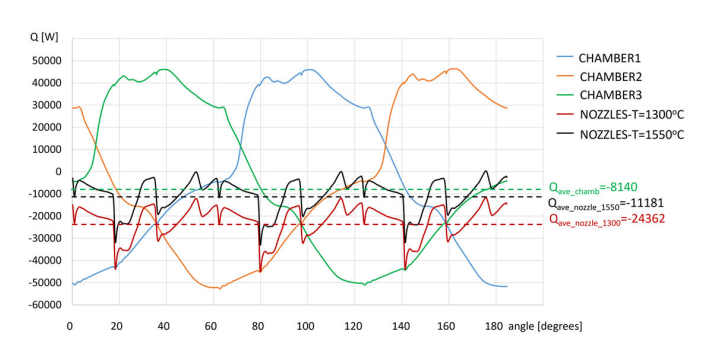


Fig. 15. Change of heat flux for wall temperature of chambers set to T = 1300°C, wall temperature of nozzles set to T = 1300°C and T = 1550°C

The first solution to this problem was the implementation of the ribs around nozzles, providing intensified zonal cooling. This caused the enhanced cooling of nozzles up to 15 200 W (see temperature distribution of the model with zonal ribs in Fig. 16).

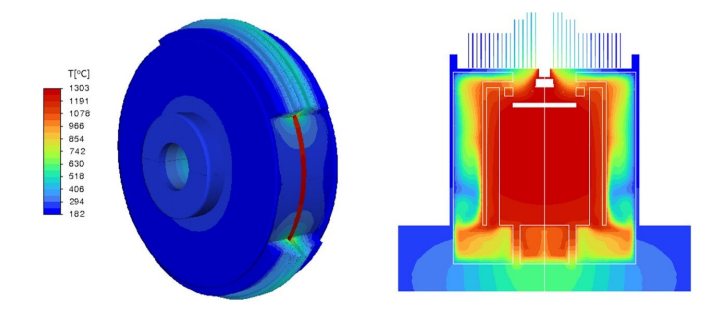


Fig. 16. Temperature distribution of engine construction with nozzles and zonal ribs

The second solution was making the nozzles with material resistant to higher temperatures, e.g., Al2O3 has a maximum working temperature of 1550°C [29] or even 1650°C [30]. This remedy lowered the required cooling heat flux to 11 181 W (Fig. 15). In that case, the nozzles should be divided into two elements. The internal casing (3–4 mm) should be made of SiN4, whereas the external part of the nozzles should be made of Al2O3 (see Fig. 17). The second option is the entire nozzle made of Al2O3. The choice of the variant will depend on the size of the real deformation and its influence on sealing effectiveness. It is worth mentioning that Si3N4 has a low thermal expansion

coefficient $(3.2 \cdot 10^{-6}/^{\circ}\text{C})$, whereas Al2O3 has a bigger thermal expansion coefficient $(8 \cdot 10^{-6}/^{\circ}\text{C})$. The temperature distribution for 1550°C prescribed to the internal surface of nozzles is presented in Fig. 19. The heat flux of nozzles cooling was equal to 10050 W, which was close to the heat flux obtained with simulation model of engine operation (Fig. 2), which was equal to 11181 W (Fig. 15). The nozzles may be a single cylindrical element (variant 1), or the nozzles may consist of two elements inserted from above (variant 2) (Fig. 17). From the point of view of assembly, the better choice is the insertion of nozzles from above, which is shown in Fig. 18.

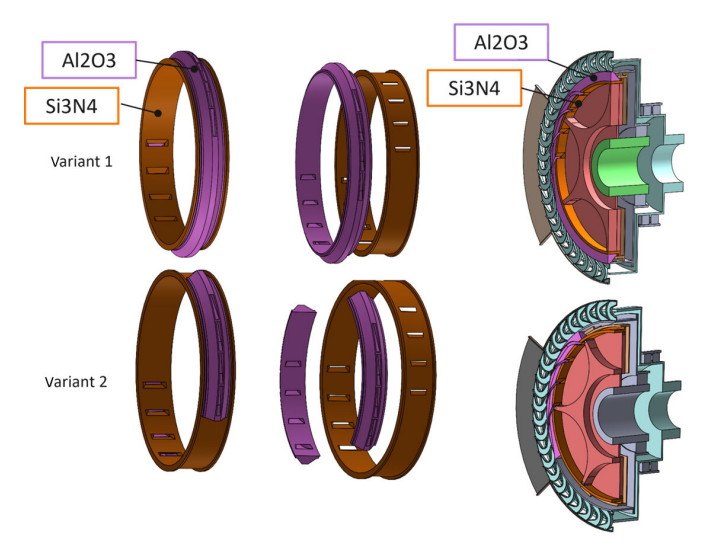


Fig. 17. Construction of nozzles made with two different ceramic materials

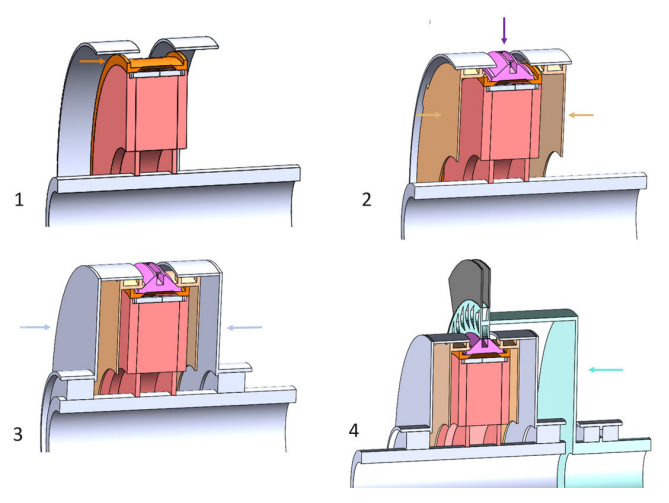


Fig. 18. Engine components assembly steps

The final simulation model, in addition to the nozzles, also contained the rotating shaft of the turbine and additional heat flux coming from the cooling of these components. The speed of the shaft was equal to 35 000 rpm. The air in the cavity between the shaft and the aluminum body had a velocity in the range of 100–799 m/s. The velocity distribution of air is presented in Fig. 20.

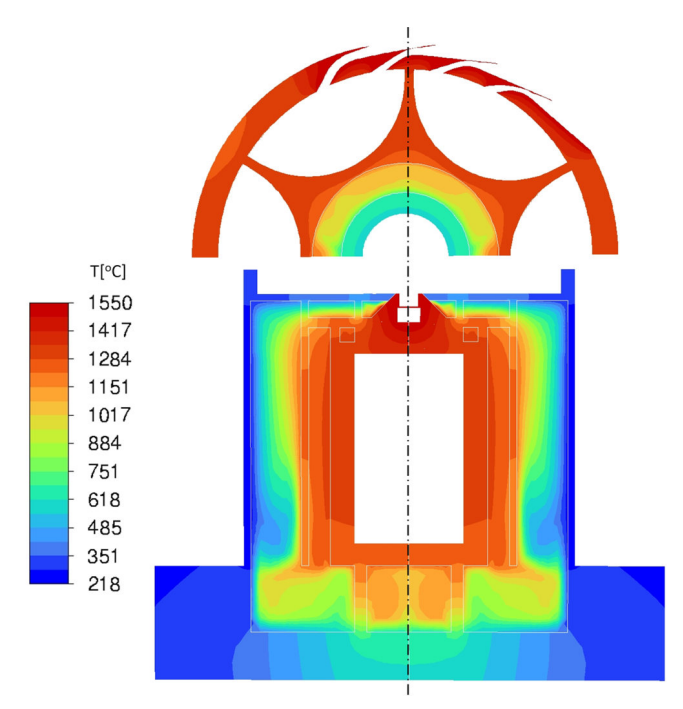


Fig. 19. Temperature distribution for nozzles at a temperature of $1550^{\circ}C$

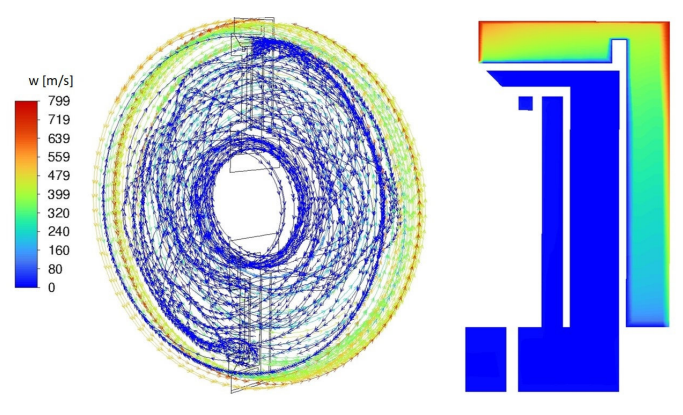


Fig. 20. Velocity distribution of air in cavity

Outstanding cooling properties of the aluminum body were observed, despite it being closed in the shaft. The reason for this was the extremely high velocity of air, which intensified heat transfer by convection. The temperature of the aluminum body on both sides of the chambers was almost the same (see Fig. 21). This means that the cooling performance on both sides of the engine was similar.

The maximum temperature of the cast iron casing and screen was around the permissible operating temperature of 1100°C. The outer body made of an aluminum alloy reached a maximum temperature of about 400°C, which is close to the permissible temperature for this material [31–33].

The heat flux of the cooling turbine reached 7140 W, which matched the model in Fig. 2. The sum heat flux from combustion chambers, nozzles, and the turbine was equal to 3.84% of the chemical energy of fuel (see Table 1).

Material and technological concept of the construction of a turboshaft engine with the application of isochoric combustion...

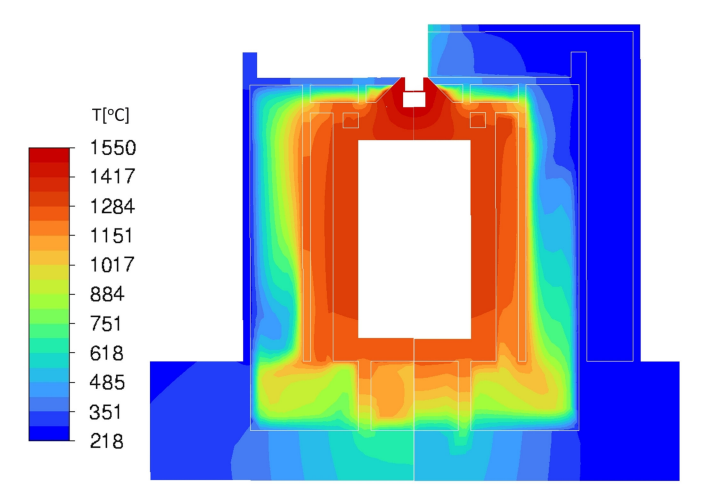


Fig. 21. Temperature distribution of engine construction with nozzles and turbine shaft

Table 1 Comparison of cooling heat flux results for the CFD model of engine operation and the CFD model of structure cooling

Part of the engine	CFD model of engine operation Heat flux [W]	CFD model of construction cooling Heat flux [W]	Ratio of cooling flux to engine chemical energy
Chambers	16 280	16 032	1.18%
Nozzles	22 362	20 100	1.62%
Turbine	14 400	14 280	1.043%
SUM	53 042	50 412	3.84%

The intensification of cooling would be further increased by the installation of additional ribs on nozzles, which is shown in Fig. 22.

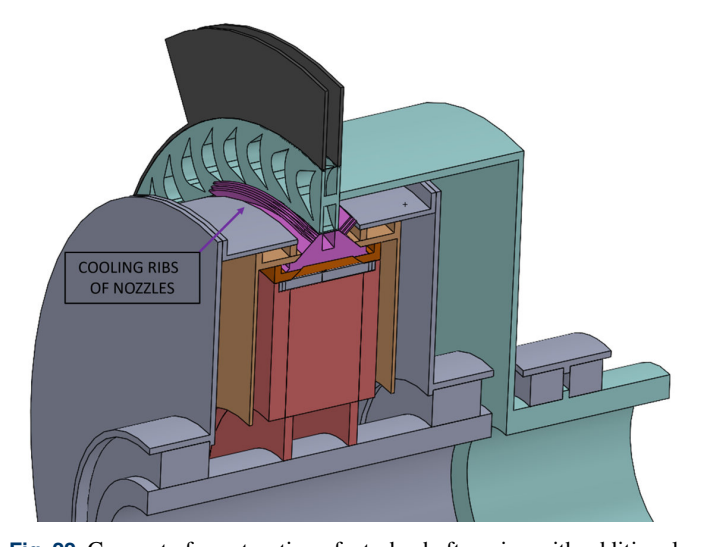


Fig. 22. Concept of construction of a turboshaft engine with additional cooling ribs of the nozzle

6. CONCLUSIONS

The paper presents a turboshaft engine concept (500 kW) using isochoric combustion. Its effective efficiency of 0.318 is incredibly promising. It achieves better results than comparable power commercial turboshaft engines currently on the market [16].

It is worth mentioning the simplicity of the presented engine concept. It consists of a two-stage compression (turbo-compressor and centrifugal compressor). Only two sets of high-pressure injection systems are required. The power is generated in a one-stage turbine. Moreover, the injection system and turbochargers available in the automotive market can be adopted.

The conducted thermal analysis of the concept of construction and selection of materials showed that it is possible to design an engine with low thermal losses and with a compact design. To reduce heat loss, the following actions were conducted:

- The use of ceramic materials with high working temperatures.
- Reducing conduction heat transfer by limiting the contact area of the ceramic chambers with the shaft, the ceramic casing with the cast iron casing, and the cast iron casing with the cast iron body.
- Reducing radiative heat transfer by the implementation of screens.
- Reducing radiative heat transfer by polishing the surfaces (reduction of the emissivity factor).

The heat losses obtained with the simulation model of engine operation (Section 3) matched the thermal construction simulation model (Section 5). The sum heat flux of cooling of combustion chambers, nozzles, and turbines was equal to 3.84% of the chemical energy of fuel, which is extremely low value.

The proposed self-adjusting segmented ceramic sealing system is a critical point in the design of an engine with the application of isochoric combustion chambers. Thus, the next primary step should be experimental verification of the sealing system. It could be done using the concept of the construction of the valve timing system, developed in Section 4. This is an optimal design since it allows the tightness of combustion chambers with the required lowest possible costs.

Full tightness of seals is key to successfully implementing isochoric combustion in the presented engine concept. Successful verification of the sealing system may open the door to the construction of this type of engine.

The concept of construction of the engine, presented in Section 5, ensured that materials could work below permissible temperatures. The analysis conducted in the paper using two different CFD models demonstrated that it was possible to construct this kind of engine with promising high efficiency.

ACKNOWLEDGEMENTS

The article was co-financed from the state budget of Poland and awarded by the Minister of Science within the framework of the Excellent Science II Programme.

REFERENCES

[1] A. Fayez, "Electric Vehicles: Benefits, Challenges, and Potential Solutions for Widespread Adaptation," *Appl. Sci.*, vol. 13, no. 10, p. 6016, 2023, doi: 10.3390/app13106016.

- [2] S.S. Ahangar, S.R. Abazari, and M. Rabbani, "A region-based model for optimizing charging station location problem of electric vehicles considering disruption A case study," J. Clean. Prod., vol. 336, no. 15, p. 130433, Feb 2022, doi: 10.1016/j.jclepro.2022.130433.
- [3] J. Konieczny et al., "Hydrogen or Electric Drive-Inconvenient (Omitted) Aspects," Energies, vol. 16, no. 11, p. 4400, 2023, doi: 10.3390/en16114400.
- [4] A. Kuśmierek, C. Galiński, and W. Stalewski, "Review of the hybrid gas - electric aircraft propulsion systems versus alternative systems," *Prog. Aerosp. Sci.*, vol. 141, p. 100925, Aug 2023, doi: 10.1016/j.paerosci.2023.100925.
- [5] P. Ackermann *et al.*, "Designed to Be Green, Economic, and Efficient: A Ketone-Ester-Alcohol-Alkane Blend for Future Spark-Ignition Engines," *ChemSusChem*, vol. 14, no. 23, pp. 5254–5264, Oct. 2021, doi: 10.1002/cssc.202101704.
- [6] R. Lin, C. Deng, W. Zhang, F. Hollmann, and J.D. Murphy, "Production of Bio-alkanes from Biomass and CO₂," *Trends Biotechnol.*, vol. 39, no. 4, Apr 2021, doi: 10.1016/j.tibtech.2020.12.004.
- [7] C. Brophy and G. Roy, "Benefits and Challenges of Pressure-Gain Combustion Systems for Gas Turbines," *Mech. Eng.*, vol 131, no. 3, pp. 54–55, Mar 2009, doi: 10.1115/1.2009-MAR-8.
- [8] K. Kurec, J. Piechna, and K. Gumowski, "Investigations On Unsteady Flow within a Stationary Passage of a Pressure Wave Exchanger by Means of PIV Measurements and CFD Calculations," *Appl. Therm. Eng.*, vol. 112, no. 5, pp. 610–620, Feb 2017, doi: 10.1016/j.applthermaleng.2016.10.142.
- [9] P. Akbari and M.R. Nalim, "Review of Recent Developments in Wave Rotor Combustion Technology," *J. Propuls. Power.*, vol. 25, no. 4, pp. 833–844, Jul 2009, doi: 10.2514/1.34081.
- [10] F. Walraven, "Operational Behavior of a Pressure Wave Machine with Constant Volume Combustion," ABB Technical Report CHCRC 94-10, 1994, Tatarstan, Russia, Sep 11–13, 2007.
- [11] P. Akbari, C. Tait, and G. Brady, "Enhancement of the Radial Wave Engine," AIAA P&E, 2019 Forum, Cincinnati, Aug 2019, doi: 10.2514/6.2019-4037.
- [12] J. Piechna, "A Review of Shock Wave Compression Rotary Engine Projects, Investigations and Prospects," *Energies*, vol 15, no. 24, p. 9353, Dec 2022, doi: 10.3390/en15249353.
- [13] P. Tarnawski, "Pulse Powered Turbine Engine Concept," Ph.D. dissertation, Faculty of Automotive and Construction Machinery Engineering, Warsaw University of Technology, 2018.
- [14] P. Tarnawski and W. Ostapski, "Pulse Powered Turbine Engine Concept Implementing Rotating Valve Timing System: Numerical CFD Analysis," *J. Aerosp. Eng.*, vol. 32, no. 3 Feb 2018, doi: 10.1061/(ASCE)AS.1943-5525.0001.
- [15] P. Tarnawski, "The hybrid concept of turboshaft engine Working according to Humphrey cycle dedicated to variety power demand CFD analysis," *Combust. Engines*, vol. 193, no. 2, pp. 129–136, May 2023, doi: 10.19206/CE-162763.
- [16] Gas Turbine Engines. "Aviation week and space Technology." [Online] Available: http://www.geocities.jp/nomonomo2007/Air craftDatabase/AWdata/AviationWeekPages/GTEnginesAWJan 2008.pdf (Accessed: 11.11.2022).
- [17] P. Tarnawski and W. Ostapski, "Rotating combustion chambers as a key feature of effective timing of turbine engine working according to Humphrey cycle CFD analysis," *Bull. Pol. Acad.*

- Sci. Tech. Sci., vol. 70, no. 5, p. e143100, Oct 2022, doi: 10.24425/bpasts.2022.143100.
- [18] P. Tarnawski and W. Ostapski, "The Hybrid Concept of Turboshaft Engine Enhanced by Steam Cycle Using Waste Heat Recovery – Combined Analytical and Numerical Calculation of Its Efficiency," SAE Int. J. Engines, vol 17, no. 6, Jun 2024, doi: 10.4271/03-17-06-0045.
- [19] S. Hong *et al.*, "Optimization sealing and cooling to control gas intrusion in a floating-wall combustion chamber," *Bull. Pol. Acad. Sci. Tech. Sci.*, vol. 72, no. 2, p. e148836, Mar 2024, doi: 10.24425/bpasts.2024.148836.
- [20] K. Chidambaram and T. Packirisamy, "Smart ceramic materials for homogeneous combustion in internal combustion engines – A review," *Therm. Sci.*, vol. 13, no. 3, pp. 153–163, 2009, doi: 10.2298/TSCI0903153C.
- [21] A. Oziębło, K. Perkowski, I. Witosławska, M. Gizowska, M. Osuchowski, and A. Witek, "Mechanical properties of silicon nitride (Si3N4) sintered under isostatic pressure and free-sintered – comparative analysis," *Glass Ceram. (Szklo Ceramika)*, no. 1, 2014 (in Polish).
- [22] T. Jackowski, M. Elfner, and J.H. Bauer, "Experimental Study of Impingement Effusion-Cooled Double-Wall Combustor Liners: Thermal Analysis," *Energies*, vol. 14, no. 16, p. 4843, Aug 2021, doi: 10.3390/en14164843.
- [23] ANSYS®Academic Associate CFD, "Theory Guide", Release 16.2, Help System; ANSYS, Inc.: Canonsburg, PA, 2016.
- [24] J. Rączka and W. Sakwa, "Cast Iron, Engineer's Handbook (Żeliwo, Poradnik inżyniera)," Odlewnictwo, WNT, vol. I, pp. 1-201, Warszawa, 1986 (in Polish)
- [25] L. San Andrés, "Gas labyrinth seals: on the effect of clearance and operating conditions on wall friction factors a CFD investigation," *Tribol. Int.*, vol. 131, pp. 363–376, Mar 2019, doi: 10.1016/j.triboint.2018.10.046.
- [26] B. Przybyła and Z. Zapałowicz, "Review of sealing methods," Scientific Papers of the Rzeszów University of Technology, 2015.
- [27] A.V. Murray, P.T. Ireland, and E. Romero, "Development of a Steady-State Experimental Facility for the Analysis of Double-Wall Effusion Cooling Geometries," *J. Turbomach.*, vol. 141, no. 4, Apr 2019, doi: 10.1115/1.4041751.
- [28] M. Martiny, A. Schulz, and S. Wittig, "Effusion Cooled Combustor Liners of Gas Turbines-An Assessment of the Contributions of Convective, Impingement, and Film Cooling," in *Proc. Symp. Energy Eng. in the 21st Century (SEE2000)*, China, 2000, pp. 221–228, doi: 10.1615/SEE2000.210.
- [29] Topseiko. "Aluminum Oxide (Al2O3) Custom Parts Machining." [Online.] Available: https://top-seiko.com/pl/works/ material-cat/ceramics/alumina/ (Accessed: 24.08.2024).
- [30] Ceramit. "Ceramic Engineering." [Online.] Available: https://www.ceramit.pl/uploads/PDFy/Ceramit_Al2O3.pdf (Accessed: 24.09.2024)
- [31] P. Pawlak, "Effects of strain rate on the instability of the PLC effect in model Al-Mg alloys," Eng. Thesis, Warsaw University of Technology, 2012.
- [32] M. Prewendowski, "High-temperature deformation of an ironaluminide-based alloy," Ph.D. dissertation, Silesian University, Katowice 2013.
- [33] ASM International. "Metals Handbook" Desk Edition, 1998.